Biomaterials 311 (2024) 122666

Contents lists available at ScienceDirect

Biomaterials

journal homepage: www.elsevier.com/locate/biomaterials

Self-assembled protein vesicles as vaccine delivery platform to enhance antigen-specific immune responses

Yirui Li [a], Mariela R. Rodriguez-Otero [a,b], Julie A. Champion [a,b,*]

[a] BioEngineering Program, Georgia Institute of Technology, USA
[b] School of Chemical and Biomolecular Engineering, Georgia Institute of Technology, USA

ARTICLE INFO

Keywords:
Nanoparticle
Vaccine
Vesicle
Elastin-like polypeptide

ABSTRACT

Self-assembling protein nanoparticles are beneficial platforms for enhancing the often weak and short-lived immune responses elicited by subunit vaccines. Their benefits include multivalency, similar sizes as pathogens and control of antigen orientation. Previously, the design, preparation, and characterization of self-assembling protein vesicles presenting fluorescent proteins and enzymes on the outer vesicle surface have been reported. Here, a full-size model antigen protein, ovalbumin (OVA), was genetically fused to the recombinant vesicle building blocks and incorporated into protein vesicles via self-assembly. Characterization of OVA protein vesicles showed room temperature stability and tunable size. Immunization of mice with OVA protein vesicles induced strong antigen-specific humoral and cellular immune responses. This work demonstrates the potential of protein vesicles as a modular platform for delivering full-size antigen proteins that can be extended to pathogen antigens to induce antigen specific immune responses.

1. Introduction

Vaccines play a vital role as public health interventions against infectious diseases [1,2]. Traditional vaccines consist of live attenuated or inactivated virus [3,4]. Although these whole pathogen vaccines elicit strong and long-lasting protective immune response, they do not offer efficient protection against some diseases and are not safe for immunocompromised persons. Protein subunit vaccines, which only include selected antigens from pathogens, offer a safe alternative to live attenuated and inactivated viruses [5,6]. Moreover, subunit vaccines enable control over antigen-specific immune response, and they are easier to manufacture compared to traditional vaccines. However, subunit vaccines are generally limited by weak and short-lived humoral and cellular immune responses. Therefore, subunit vaccines are often required to be co-administered with adjuvants or in delivery systems for sufficient immune response [7,8].

In recent decades, nanoparticle delivery systems have been widely studied for subunit vaccine delivery [8–11]. Nanoparticles offer several beneficial features, which include multivalent antigen display to B cell receptors, enhanced uptake by antigen presenting cells, protection of the antigen against degradation, and co-delivery of antigens and adjuvants. Liposomes, polymeric nanoparticles, and protein nanoparticles are commonly investigated for subunit vaccine delivery [12–14]. In liposome and polymeric nanoparticle systems, antigens are either encapsulated within the core or conjugated on the surface. However, both systems face the challenges of low antigen encapsulation and denaturation of antigens during fabrication or chemical conjugation [11,15,16]. Virus like particles (VLPs) are the only FDA approved protein nanoparticle for vaccination [17,18]. As they are made from viral coat proteins, they are quite immunogenic but also introduce off target antigens from the VLP scaffold itself, thereby reducing the control over antigen specificity that is often desired in a subunit vaccine. A number engineered protein nanoparticles have been developed to improve control over both antigen presentation and physical properties [14]. Protein nanoparticles can be formed via desolvation or self-assembly. In the desolvation process, organic solvents may denature antigen proteins, thereby hampering their ability to induce humoral immune responses [19,20]. In self-assembling protein nanoparticle systems, antigens are genetically fused to protein or peptide building blocks to display antigens on the surface [14,21]. Self-assembling systems are beneficial for vaccine delivery because they mimic the multivalent, oriented antigen display and the size of natural pathogens (~20 nm–400 nm) while preserving the selectivity of subunit vaccines. Furthermore, self-assembly in aqueous buffer better maintains the structure of antigen

* Corresponding author. 950 Atlantic Drive NW, Atlanta, GA, 30332, USA.
E-mail address: julie.champion@chbe.gatech.edu (J.A. Champion).

https://doi.org/10.1016/j.biomaterials.2024.122666
Received 7 September 2023; Received in revised form 18 May 2024; Accepted 11 June 2024
Available online 12 June 2024

proteins. Self-assembling peptide cages (SAGEs) and self-assembling protein nanoparticle (SAPNs) are two examples of self-assembling systems for subunit vaccine delivery [22–26]. Both systems have shown efficacy to provide protection against infectious disease in animal models. However, only antigenic peptides and very small proteins, such as 32 amino acid Helix C of influenza, were genetically fused to their building blocks instead of full-sized, folded antigen proteins, as genetic fusion to larger antigen proteins may hamper self-assembly. Large protein antigens can provide broad-spectrum protection by eliciting immune responses against multiple epitopes with conformations that are identical to conformations in pathogens [27,28]. *De novo* designed icosahedral protein cages that resemble VLPs, but have no viral components, are capable of displaying large protein antigens such as DS-Cav1 from Respiratory syncytial virus and SARS-CoV-2 spike [29,30]. Additionally, a variety of natural protein cages such as human ferritin, can also be recombinantly fused to antigens, including SARS-CoV-2 spike [14,31].

In addition to SAGEs, SAPNs and protein cages, self-assembling elastin-like polypeptides (ELPs) have been explored for designing nanoparticle vaccines. ELP is a thermosensitive peptide with the typical sequence $(VPGXG)_n$ that undergoes a hydrophobic transition upon warming that leads to coacervation and phase separation [32–34]. ELP-based nanoparticle vaccines were self-assembled from ELPs that were genetically fused to antigenic peptides [35,36] or small antigen protein, M2e (23 amino acids) [37]. Recently, an ELP micelle was reported consisting of 17 kDa birch pollen allergen fused to ELP combined with excess ELP that induced antibody production and little T cell response, for potential use in subcutaneous allergen immunotherapy [38]. Our group has previously developed protein vesicles self-assembled from full-size, globular proteins, including fluorescent proteins [39] and enzymes [40]. The proteins are fused to acidic leucine zipper, Z_E, and mixed with ELP fused to basic leucine zipper, Z_R (Z_R-ELP). Z_E and Z_R bind each other with high (10^{15} M) affinity [41]. Upon warming, the proteins transition from soluble to unstable coacervates to stable, hollow vesicles [42]. Furthermore, protein vesicle diameter and membrane structure could be tuned by varying molar ratio of Z_E to Z_R [39], protein concentration [42], and NaCl concentration [43]. Inspired by these protein vesicles that display large globular proteins on their surface, we asked whether protein vesicles would be an effective, novel vaccine platform to deliver larger antigen proteins. In this study, we chose a model antigen protein, ovalbumin (OVA, 43 kDa), which is known to be immunogenic and has been commonly used to investigate the efficacy of nanoparticle vaccine platforms [44–46]. OVA was genetically fused to Z_E to incorporate OVA into protein vesicles through self-assembly. Non-natural amino acid, *para*-azidophenylalanine (pAzF) was incorporated into Z_R-ELP (pZ_R-ELP) to enable photo-crosslinking of OVA protein vesicles. To examine the efficacy of protein vesicles for vaccine delivery, we characterized the self-assembly and nanostructure of OVA protein vesicles and vaccinated mice. We sought to identify the relative strength of the humoral immune response to the OVA antigen relative to the other protein domains in the vesicle and determine the ability of protein vesicles to induce both antibody and T cell responses.

2. Materials and methods

2.1. Expression and purification of proteins

pET17b-OVA-Z_E plasmid was purchased from Genscript. *E. coli* Shuffle T7 strain (NEB) was transformed with pET17b-OVA-Z_E. To express OVA-Z_E, a single colony was inoculated in 10 mL lysogeny broth (LB) medium containing 200 mg/L ampicillin and shaken overnight at 30 °C. 30 mL overnight culture was inoculated in 1 L LB media. When optical density at 600 nm (OD600) reached ~0.8 to 1, 1 mM isopropyl-β-thiogalactoside (IPTG) was added to induce protein expression, and the culture was shaken at 16 °C for an additional 18 h. Cells were harvested by centrifugation (4000 g, 10 min) and stored at −20 °C. The pellets were resuspended in lysis buffer (300 mM NaCl, 50 mM NaH_2PO4, and 10 mM imidazole), followed by sonication for 15 min. After centrifugation (10,000 g, 30 min), the supernatant was incubated with Ni-nitrilotriacetic acid (NTA) agarose resin (Qiagen) for 1 h at 4 °C. The suspension was flowed through an Econo-Column (Biorad) and washed with 100 mL of lysis buffer containing 40 mM imidazole. Elutions were collected using buffer with 250 mM imidazole. The protein elutions were buffer exchanged into phosphate buffered saline (PBS) by dialysis with four buffer exchanges at 4 °C.

pZ_R-ELP was produced as described previously [43]. *E. coli* strain AFIQ-BL21 [47] was transformed with pQE60-Z_R-ELP containing a mutant *E. coli* phenyl-alanyl-tRNA synthetase (A294G) gene [48,49]. Briefly, a single colony was grown overnight and inoculated in 1 L M9 minimum media supplemented with glucose (0.4 wt %), thiamine (5 mg/L), MgSO4 (1 mM), CaCl2 (0.1 mM), and 20 natural amino acids at a concentration of 1 mg/L each. At OD600 of 0.8, cells were harvested by centrifugation and resuspended in M9 minimum media supplemented with 19 natural amino acids at 1 mg/L each except phenylalanine and 0.3 mg/L pAzF (Bachem). After 15 min, 1 mM IPTG was added for induction. After 5 h, cells were harvested by centrifugation and purified with Ni-NTA resin using non-native buffers as described previously [39]. Purified pZ_R-ELP was dialyzed (3k MWCO) into Milli-Q water and lyophilized. All protein sample containers were wrapped in foil and kept in the dark to protect pAzF from ambient light. Protein purity was verified by sodium dodecyl sulfate polyacrylamide gel electrophoresis (SDS-PAGE).

2.2. Vesicle assembly and turbidity measurement

Protein solutions were prepared on ice by adding water, pZ_R-ELP, and OVA-Z_E, then adding 10× PBS to achieve a specified salt concentration based on NaCl in 10× PBS. Solutions were moved to the bench (25 °C) for 1 h to induce vesicle assembly. Vesicles were crosslinked by UV irradiation at 254 nm for 30 min. The turbidity of protein solutions was measured at OD 400 nm, using a microplate reader (Synergy HT Multi-Mode, BioTek). 100 μL of protein solutions were prepared in a 96-well microplate at 4 °C and placed in the microplate reader at 25 °C. Then, the changes of turbidity were monitored by recording the OD of protein solutions every minute for 1 h.

2.3. Dynamic light scattering (DLS)

Hydrodynamic diameter and zeta potential of protein vesicles were measured by Zetasizer DLS instrument (Malvern Instruments, Malvern). A 4 mW He–Ne laser operating at a wavelength of 633 nm was equipped and operated at a detection angle of 173°. 70 μL of vesicle solution was prepared in a microcuvette and hydrodynamic diameter was measured at 25 °C. The solvent was adjusted to aqueous solutions containing 0.50 M–1.5 M NaCl buffered with phosphate and the material was protein. Z-average values were used to report vesicle size. The zeta potential was measured using a folded capillary cell and the protein vesicle sample was adjusted to aqueous solution containing 0.1× PBS.

2.4. Transmission electron microscopy (TEM)

OVA protein vesicles were imaged by a TEM (JEM 100CX-II, JEOL). 5 μL of protein vesicle solution was dropped on a copper grid (Electron Microscopy Sciences) for 5 min at 25 °C, washed with Milli-Q water, stained with 1 % phosphotungstic acid solution for 20 s, and washed with Milli-Q water. TEM samples were air-dried for 24 h and imaged at 100 kV.

2.5. Circular Dichroism (CD)

The CD spectra of soluble OVA-Z_E and photo-crosslinked OVA

protein vesicles were obtained by Chirascan-plus CD spectrometer (Applied Photophysics). Measurements were performed in a 0.2 cm length cuvette at 25 °C. The spectra were obtained in 1 nm increments within a wavelength range of 200–280 nm.

2.6. Enzyme-linked immunosorbent assay (ELISA)

ELISA was performed to determine OVA-specific antibody affinity and accessibility of OVA protein on vesicles. Maxisorp 96 well immune assay plates (Nunc) were coated with 1 μg/mL of OVA protein vesicles in PBS at 25 °C overnight. Each well was blocked with 100 μL of 1 % bovine serum albumin (BSA) in PBS containing 0.05 % v/v Tween 20 (PBST) at 25 °C for 1 h. Plates were washed, and each well was incubated with serially diluted OVA Polyclonal Antibody (Thermo Fisher Scientific) at 25 °C for 1 h. After incubation, each well was washed and incubated with 160 ng/mL of horseradish peroxidase (HRP)-conjugated goat anti-rabbit IgG secondary antibody (Thermo Fisher Scientific) at 25 °C for 1 h. Plates were washed again, followed by the addition of 50 μL 3,3′,5,5′ tetramethylbenzidine (TMB) to each well. The enzymatic activity of HRP was stopped by addition of 50 μL H_2SO_4 to each well. Optical density was measured at 450 nm and 570 nm for background subtraction.

2.7. Endotoxin removal

Endotoxin levels in OVA-Z_E and pZ_R-ELP were reduced by Pierce™ High Capacity Endotoxin Removal Resin (Thermo Fisher). To confirm low endotoxin content within proteins, the endotoxin levels in OVA-Z_E and pZ_R-ELP were quantified by ToxinSensor™ Chromogenic LAL Endotoxin Assay Kit (GenScript). OVA-Z_E and pZ_R-ELP with low endotoxin levels and endotoxin free water, PBS, and saline were used to prepare OVA protein vesicles for *in vitro* and *in vivo* studies. The endotoxin level in all samples was less than 5 EU/kg as recommended by the United States Pharmacopoeia [50].

2.8. In vitro dendritic cell assessment

The JAWS II immature dendritic cell (DC) line (ATCC) was cultured in MEM-alpha (Corning) supplemented to 4 mM glutamine and 5 ng/mL GM-CSF (Peprotech), 20 % fetal bovine serum (FBS), and 1 % penicillin/streptomycin (Amresco). JAWS II DCs were plated in 48-well plates for measuring *in vitro* maturation. Cells were stimulated with 5 μg/mL of bacterial lipopolysaccharide (LPS) and 20 μg/mL of soluble OVA, soluble OVA-Z_E or OVA protein vesicles. After 24 h, cells were fixed with 3.7 % paraformaldehyde and blocked with 1 % BSA in PBS for 1 h. Next, cells were incubated with 1 μg/μL of TruStain FcX antibody (BioLegend) for 10 min on ice to block non-specific binding to Fc receptors. After that, cells were stained with 1 μg/μL of PE anti-mouse CD86 (BioLegend) for 30 min. Finally, cells were washed twice with PBS and scraped from the plate. The upregulation of CD86 was analyzed by flow cytometry.

2.9. Immunization of mice

All animals were treated in accordance with the regulations and guidelines of the NIH Guide for the Care and Use of Laboratory Animals, and all protocols and procedures were reviewed and approved by Georgia Tech's Institutional Animal Care and Use Committee (A100529). 6-8 week-old Balb/c mice (Jackson Laboratory) were immunized intramuscularly at the right back leg with solutions containing 10 μg of soluble or vesicle form of OVA-Z_E in pharmaceutical grade saline. Prime vaccination was given at day 0 and booster vaccination was given at day 21. Animals were monitored for weight loss and signs of lethargy after vaccination for 7 days.

2.10. Blood collection

Approximately 100 μL of blood was collected from immunized mice by jugular vein puncture immediately prior to vaccination and 2 weeks after prime and boost vaccinations. Blood was allowed to clot in BD Vacutainer tubes (Becton, Dickinson & Company) and was centrifuged at 1000 g for 15 min to collect serum. Serum was stored at −20 °C.

2.11. Antibody endpoint titer measurement

Nunc MaxiSorp plates (Thermo Fisher) were coated with 1 μg/mL of purchased OVA (Sigma) in PBS overnight at room temperature. Plates were blocked with 1 % BSA in PBST for 1 h followed by three washes with PBST. Next, serum was added at a 1/10 dilution and subsequent 5-fold serial dilutions in 1 % BSA/PBST and incubated for 1 h at room temperature. Serum from naïve mice (pre-vaccination) was also run on each plate to determine cutoff values. After serum incubation, plates were washed with PBST and incubated with HRP-conjugated goat anti-mouse IgG1 antibodies (Southern Biotech) or HRP-conjugated goat anti-mouse IgG2a-HRP antibodies (Southern Biotech) at a 1:4000 dilution in 0.1 % BSA/PBST for 1 h at room temperature followed by washing with PBST. 100 μL TMB chromogen solution (Thermo Fisher) was added into each well. After 30 min, the enzymatic reaction was quenched with H_2SO_4 (Thermo Fisher). OD was read at 450 nm using a microplate reader (BioTek). End point titers were determined from reciprocal dilutions to determine the dilution at which the OD value was equal to the mean + three standard deviations of that of naïve serum [51]. Titer values too low for detection were fixed at 10, corresponding to the lowest dilution used.

2.12. Preparation of splenocytes and lymphocytes

2 weeks after boost immunization, mice were sacrificed by euthanasia, and spleens were collected. Spleens were manually homogenized by the plunger of a 3 mL syringe (Becton, Dickinson & Company) in a 100 μM cell strainer (Greiner Bio-One). Single cell suspensions of splenocytes were prepared by forcing cells through cell strainers with complete RPMI media (RPMI, 2 mM L-Glutamine, 50 μM 2-mercaptoethanol, 100 U/mL penicillin, 100 μg/mL streptomycin, and 10 % FBS). Cells were centrifuged at 350 g for 5 min. Splenocytes were resuspend in 1 mL ACK lysing buffer (Thermo Fisher) to lyse red blood cells. After 10 min, splenocytes were centrifuged and resuspended in complete RPMI media.

2.13. Intracellular cytokine staining

Splenocytes were plated in 96-well U-bottom plates at 10^6 cells/well in RPMI and stimulated with 1 μg/mL of PepTivator Ovalbumin (Miltenyi Biotec). After 3 h, each well was supplemented with a transport inhibitor, 1× brefeldin A (Biolegend), and incubated for an additional 3 h. Cells in each well were centrifuged at 350 g for 5 min and resuspended in 100 μL of PBS premixed with 0.5 μL of Trustain FcX plus blocking solution (BioLegend) on ice for 10 min. Cells were centrifuged and stained by 100 μL of antibody cocktail solution containing Zombie Violet, PerCP anti-mouse CD3ε antibody, FITC anti-mouse CD8a antibody and APC/Cyanine7 anti-mouse CD4 antibody (BioLegend) in PBS. After staining for 1 h in the dark, cells were washed with 1 % BSA in PBS, centrifuged, and fixed with 100 μL of 3.7 % formaldehyde (VWR) in PBS for 30 min on ice. After fixation, cells were centrifuged and washed once with 100 μL of permeabilization buffer (eBioscience). Cells were centrifuged and resuspended in 100 μL of permeabilization buffer containing 1.5 μL of PE anti-mouse IFN-γ antibody and 1.5 μL of PE/Cyanine7 anti-mouse IL-4 antibody. After incubation on ice for 30 min, cells were centrifuged, washed with 1 % BSA in PBS, and resuspended in 100 μL of 1 % BSA in PBS. Flow cytometry analysis was conducted using Cytek Aurora (Cytek Biosciences). Data was analyzed with Flow Jo (Becton, Dickinson & Company).

2.14. Statistical analysis

Antibody endpoint titers were analyzed using the Mann–Whitney *U* test and T cell counts were analyzed by one-way analysis of variance (ANOVA) with Tukey's post-hoc multiple comparison. All statistical analysis were conducted using GraphPad Prism 9 (GraphPad). The p values < 0.05 were considered statistically significant (*$p < 0.05$, **$p < 0.01$, ***$p < 0.005$, ****$p < 0.001$).

3. Results and discussion

3.1. Synthesis of recombinant OVA-Z_E and pZ_R-ELP

OVA-Z_E was expressed in the Shuffle T7 express strain, which is an engineered *E. coli* strain to promote disulfide bond formation in the cytoplasm [52], and the final yield was ~1 mg/L of *E. coli* culture (Figs. S1a and S1b). To verify that fully folded OVA was produced, we compared the secondary structure of recombinant OVA-Z_E with native OVA measured by circular dichroism (CD). According to the CD spectra (Fig. S1c), OVA-Z_E showed similar, but slightly different structure from native OVA, likely due to the fusion to Z_E motif and lack of post-translational modification. *E. coli* expression does not provide native post-translational modifications to viral (or egg) proteins, and it is challenging to express antigens with complex structures. Furthermore, endotoxin contamination requires extra processing steps after antigen production. Therefore, insect cells or mammalian cells can be used for antigen protein expression in future work, as is common in subunit viral vaccines [53]. The second component of vesicles is Z_R-ELP. To stabilize protein vesicles, a photo-crosslinkable non-natural amino acid, pAzF, was incorporated into phenylalanine residues in the ELP domain by the global incorporation method using phenylalanine auxotroph AFIQ *E. coli* containing a mutant phenylalanyl-tRNA synthetase, as described previously [43,49,54]. UV crosslinking creates covalent bonds between the azide group and nearby protein backbone, as evidenced by oligomers of pZ_R-ELP seen in SDS-PAGE (Fig. S2).

3.2. Tunable size and antigen loading of OVA protein vesicles

To prepare OVA protein vesicles, 0.3–4.5 μM OVA-Z_E and 30 μM pZ_R-ELP were mixed in PBS buffer containing 0.5–1.0 M NaCl at 4 °C. Increasing the temperature to 25 °C triggered the ELP phase transition and OVA-Z_E/pZ_R-ELP complexes self-assembled into OVA protein vesicles (Fig. 1). The turbidity profiles of protein mixtures during the thermal phase transition were measured (Fig. S3). The initial rapid increase in turbidity indicated occurrence of the ELP phase transition in the protein mixtures and self-assembly and growth of particulate-like coacervates. Once the turbidity profile reached saturation it stabilized, indicating that the coacervates reorganized so that the hydrophilic OVA-Z_E shielded the hydrophobic ELP interior, resulting in the formation of stable OVA protein vesicles.

Previous work on protein vesicles has shown that the sizes could be tuned by changing NaCl concentration [43] or Z_E/Z_R molar ratio [40]. To optimize OVA protein vesicles for vaccination, DLS was used to measure hydrodynamic diameter of vesicles formed at different NaCl concentrations and Z_E/Z_R molar ratios. Increasing NaCl concentration, at constant protein concentration, increases ELP hydrophobicity [55], resulting in more compact ELP conformation. This leads to decreased vesicle sizes as the relative size of OVA to ELP increases and increased curvature is required to relieve steric constraints of OVA packed closer together due to smaller interior ELP domains (Fig. 2a). We have observed this trend with vesicles made from several other globular proteins [40]. Increasing the Z_E/Z_R molar ratio, at constant pZ_R-ELP and NaCl concentration, led to changes in the molecular packing of the protein amphiphiles. A greater number of hydrophilic OVA proteins increased the curvature of protein vesicles to accommodate steric hindrance between OVA as the Z_E/Z_R molar increased from 0.01 to 0.1 (Fig. 2b). This effect saturates at a Z_E/Z_R ratio of 0.15. We have observed previously that increasing the molar ratio beyond a critical level results in a population of soluble globular proteins co-existing with vesicles [56]. However, DLS data gave no evidence for soluble protein for 0.15 Z_E/Z_R ratio (Fig. S4). The correlogram did show that the concentration of vesicles for 0.15 Z_E/Z_R ratio was slightly less than that for 0.1, suggesting there may be protein inside the vesicles. To assess the impact of Z_E/Z_R ratio on surface antigen availability, we performed an ELISA binding experiment, using anti-OVA antibody as a probe for folded, surface accessible OVA on vesicles (Fig. 2c). Although the surface accessible OVA increases from 0.01 to 0.1 Z_E/Z_R molar ratio, there is a reduction in anti-OVA binding for vesicles made with 0.15 Z_E/Z_R ratio, which points to OVA being either inside the vesicle or aggregated or misfolded on the surface. Also, TEM of 0.15 Z_E/Z_R shows high protein density around the perimeter of the vesicles (Fig. S5). At 1 M NaCl, it is possible that both the hydrophobic ELP and the high salt itself combined with higher OVA concentrations to induce interactions that prevented complete vesicle organization from the coacervate stage, thus trapping or misfolding some OVA on the ELP side of the vesicle membrane. Altogether, this data is consistent with previous data on protein vesicles made with other globular proteins and confirms that vesicle size can be tuned. The ability to tune the density of antigen proteins on the vesicle surface is dependent on the vesicle size, and for a given salt concentration there is a limit. Antigen density is highly relevant to vaccine design and future work could explore how antigen density can be best matched to B cell receptor binding for the greatest antibody response. As small size is important for nanoparticle vaccines to enable trafficking to lymph nodes and effective uptake by antigen presenting cells (APCs), we selected nanoscale vesicles made at 0.1 Z_E/Z_R molar ratio and 1.0 M NaCl for further characterization and vaccination.

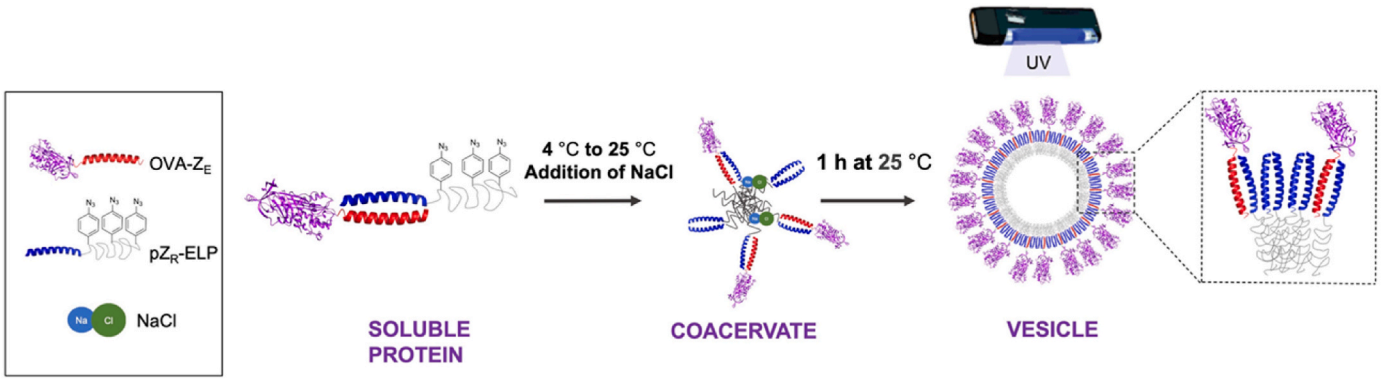

Fig. 1. Schematic of thermally triggered self-assembly of OVA protein vesicles. OVA-Z_E and pZ_R-ELP were mixed in phosphate buffer containing additional NaCl at 4 °C. Protein mixtures were then incubated at 25 °C for 1 h for vesicle self-assembly and crosslinked by UV irradiation at 254 nm for 30 min.

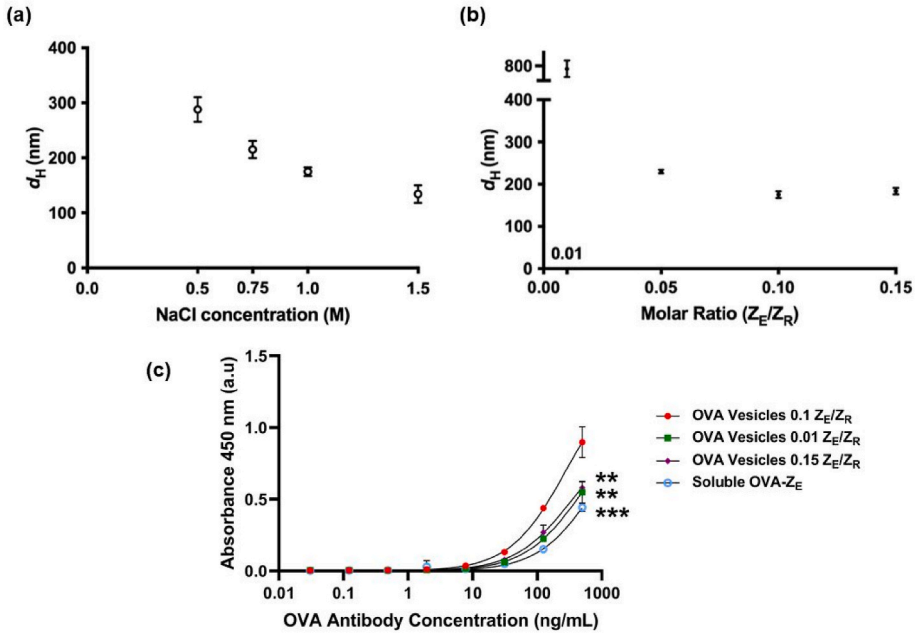

Fig. 2. Synthesis of OVA protein vesicles at various NaCl concentrations and molar ratios. (a) Hydrodynamic diameters of OVA protein vesicles formed at various NaCl concentrations with 30 μM pZ_R-ELP and 0.1 Z_E/Z_R molar ratio. (b) Hydrodynamic diameters of OVA protein vesicles formed at various Z_E/Z_R molar ratios from 30 μM pZ_R-ELP and 1.0 M NaCl. Each data point is the average of three replicate batches of vesicles. (c) Binding of anti-OVA to OVA vesicles formulated at different Z_E/Z_R ratios compared to soluble OVA-Z_E. Statistical significance is with respect to 0.1 Z_E/Z_R molar ratio vesicles. (***$p < 0.005$, **$p < 0.01$).

3.3. OVA protein vesicle characterization

Vesicles made from 30 μM pZ_R-ELP, 3 μM OVA-Z_E, and 1.0 M NaCl were crosslinked with UV irradiation at 254 nm for 30 min. This is necessary because the ELP phase transition is reversible. We previously showed that dilution of similar vesicles made with mCherry-Z_E and pZ_R-ELP at 1.0 M salt into physiological salt (0.15 M) or cooling the vesicles to 4 °C resulted in swelling and disassembly of the vesicles [42,43]. The vesicles exhibited a typical turbidity profile (Fig. S6) where upon warming the protein solution from 4 °C to 25 °C the turbidity increased and stabilized. The vesicles had a hydrodynamic diameter of 174.9 ± 8 nm with a polydispersity index of 0.2 ± 0.03 (Fig. 3a) and zeta potential of −12.8 ± 1.19 mV. TEM of OVA protein vesicles showed spherical shapes with wrinkled surface, indicative of hollow vesicle structures (Fig. 3b). To confirm UV irradiation did not denature antigen proteins on the surface, we compared the secondary structure of OVA protein vesicles with and without UV irradiation measured by CD. OVA protein vesicles with and without UV irradiation displayed comparable CD spectra (Fig. S7), which proved that UV irradiation did not damage the structure of OVA antigens on the surface. Some antigens, however, may be susceptible to denaturation by UV irradiation. In this case, the amino acid sequence of the ELP domain in Z_R-ELP can be tuned to increase the hydrophobicity and enable nanoscale vesicle assembly and stability at physiological salt concentration without crosslinking, which we have recently demonstrated [57].

To avoid hypertonic shock during *in vitro* and *in vivo* experiments, OVA protein vesicles initially formed in 1 M NaCl were dialyzed into PBS to match physiological salt concentration. Diameter of vesicles was monitored for 7 days after dialysis. OVA protein vesicles showed initial swelling to 271 nm at day 2 and were stable in PBS for 7 days (Fig. S8). Furthermore, vesicles were kept at room temperature for 44 days. Size distributions of the same sample on day 1 and day 44 proved that protein vesicles maintain their structures at room temperature at least 44 days (Fig. 3a). The long-term stability of protein vesicles at room temperature is beneficial as it can eliminate the need for high-cost cold chain shipping and storage that makes vaccines inaccessible for resource-limited regions [58,59]. However, where feasible, vaccine storage at 4 °C could be preferred and 37 °C storage data could represent hot or accelerated storage conditions and provide some insight into vesicle changes in the body. Vesicle stability was also assessed after cold (4 °C)

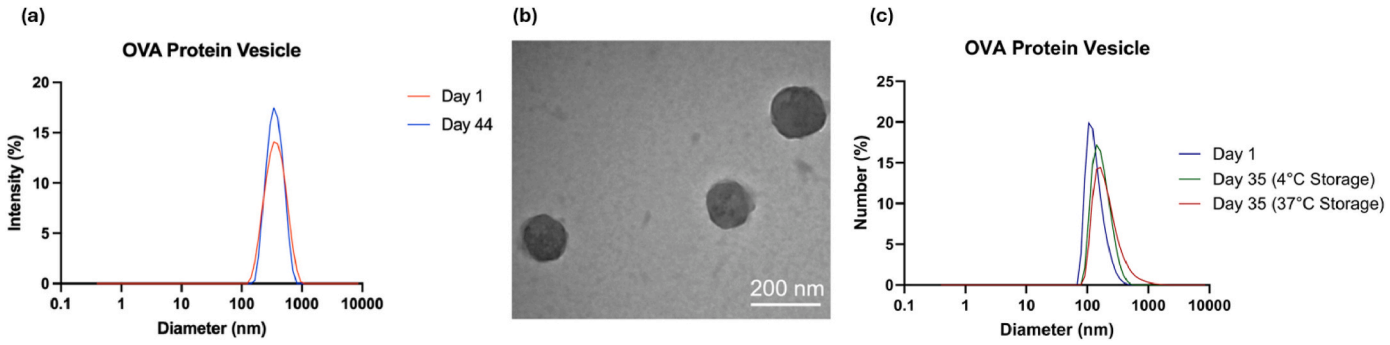

Fig. 3. Self-assembly of recombinant OVA-Z_E and pZ_R-ELP into OVA protein vesicles. (a) Size distributions of OVA protein vesicles in PBS at day 1 (red) and day 44 (blue). (b) TEM micrograph of OVA protein vesicles. Scale bar = 200 nm. (c) Size distribution of OVA protein vesicles in PBS at day 1 (blue), day 35 at 4 °C storage (green), and day 35 at 37 °C storage (red). (For interpretation of the references to colour in this figure legend, the reader is referred to the Web version of this article.)

and hot (37 °C) storage. As ELP is thermosensitive, cooling to 4 °C reverses the hydrophobic transition [42]. However, DLS indicates that vesicles maintain their size and colloidal stability after 35 days in both cold and hot storage (Fig. 3c). The size distributions are shown as Number % to identify if any soluble protein is released since the Intensity % signal is weighted towards larger particles. The lack of antigen release, even at 4 °C, is likely due to the UV crosslinking of the ELP domains to each other and femtomolar affinity between Z_E and Z_R that connects OVA-Z_E to Z_R-ELP.

Assessment of antigen integrity and surface accessibility by anti-OVA ELISA after just 1 day at 4 °C and 37 °C indicates there is no loss of anti-OVA binding (Fig. S9a). This demonstrates that even though the ELP becomes soluble at 4 °C and more hydrophobic at 37 °C, there are not changes to the vesicle organization that hide, release, or sequester the antigen. This data also suggests that upon injection into mice (37 °C), the vesicles will not undergo significant changes in structure or antigen density. CD was also used to assess the effect of storage on protein structure. Vesicles stored for 35 days at 4 °C did not show any changes in secondary structure, while vesicles stored at 37 °C exhibited a loss in molar ellipticity (Fig. S10). The fact that the vesicle diameter was stable after hot storage suggests that OVA itself suffers from loss of structure due to high temperature storage and vesicles do not prevent this. So, while vesicles may remain colloidally stable after storage at a range of temperatures, stability of the exact antigen used in the vaccine should guide storage conditions. To evaluate changes in OVA conformation or accessibility after storage, anti-OVA ELISA was performed on the cold and hot stored samples after 58 days. Fig. S9b shows that both storage conditions result in some loss of antigen integrity or accessibility, with 37 °C storage being worse than 4 °C storage, as expected based on the CD data. However, vesicles stored at both conditions still have antibody-detectable OVA on the surface. Stability will need to be assessed for each new antigen as OVA is replaced with pathogen antigens.

Similar to SAGEs, SAPNs, protein cages, and ELP micelles, OVA protein vesicles mimic the repetitive antigen display and particulate feature of natural pathogens [22–25,38]. However, SAGEs and SAPNs only showed the ability to present antigenic peptides or very small (~30 amino acids) protein on the surface. It has been challenging to genetically fuse large antigen proteins to engineered self-assembling building blocks as it can cause structural distortion in the final self-assembly [60]. So far, a few self-assembling protein nanoparticle systems have been reported to display full-size antigens [29,38,61–63]. The protein vesicle design allows presentation of full-size OVA antigens (385 amino acids) via high affinity Z_E/Z_R interactions during self-assembly and control over particle size. Furthermore, two different Z_E fusion proteins, mCherry-Z_E and GFP-Z_E, can be incorporated into the same protein vesicle [39]. This feature might be beneficial for designing multiple antigen-presenting vaccines against diseases that require vaccination with multiple antigens for comprehensive immune responses [64,65]. Matching the natural oligomeric state of some antigens is ideal for designing vaccines with enhanced immune responses, such as trimeric influenza hemagglutinin antigen [66]. Thus, trimeric coiled coils can be explored in future work as building blocks to incorporate trimeric antigens, for example [67].

Prior to immunization, we assessed the ability of vesicles to interact with dendritic cells (DCs), which play an important role as antigen presenting cells (APCs) in the early phase of adaptive immune response [68,69]. JAWS II DCs were incubated with soluble native OVA, soluble OVA-Z_E and OVA protein vesicles for 24 h. CD86 is a surface marker of DC maturation and was measured by cell labeling with fluorescent anti-CD86 antibody followed by flow cytometry [44]. Higher CD86 fluorescence in the OVA protein vesicle group indicated that OVA protein vesicles triggered the upregulation of CD86 significantly more than soluble native OVA and OVA-Z_E (Fig. S11). It has been reported that particulate nature and multivalent antigen display facilitates antigen uptake by APCs [70,71].

3.4. OVA-specific antibody responses in vivo

To assess the immune response against OVA protein vesicles, BALB/c mice were immunized intramuscularly with OVA protein vesicles and soluble OVA-Z_E in formulations containing 10 μg OVA-Z_E. The vesicle group also contained 33.8 μg pZ_R-ELP. Vesicles without antigen could not be used as a carrier control since vesicles do not form without a globular protein fused to Z_E [39]. A boost immunization of the same formulations was given on day 21 (Fig. 4). Blood samples were collected 2 weeks after prime and boost immunizations and OVA-specific antibody endpoint titers were measured by ELISA. After prime immunization, OVA protein vesicles elicited OVA-specific IgG1 and IgG2a antibody responses, while no detectable antibody response was observed in the soluble group (Fig. 5). Post boost immunization, IgG1 titers increased for both soluble and vesicle groups. However, OVA protein vesicles still showed ~20-fold higher IgG1 titer than soluble OVA-Z_E. IgG2a titers also increased in vesicle vaccinated animals after boost. No detectable IgG2a antibody response was detected in the soluble group even after boost administration. ELP micelles displaying birch pollen antigen also induced high levels of IgG1 and IgG2a, similar to alum adjuvanted antigen, though the micelle vaccine contained 36 μg antigen and was administered 3 times [38]. These results reflect the fact that multivalent antigen display on nanoparticle surfaces enhances cross-linking between B-cell surface receptors, which favors the production of antibody responses [21,72]. Therefore, it is likely that protein vesicles presenting multiple OVA antigens on the surface were advantageous for efficient binding and activation of B-cell receptors, resulting in increased antibody titers compared to soluble antigen.

Though ELPs have been proved to be immunotolerant [73–75], pZ_R-ELP in nanoparticle form may enhance immune responses against pZ_R-ELP and neutralizing antibodies against vesicles themselves may hamper the efficiency of vaccine after repetitive vaccination. Long ELPs fused to tuberculosis peptide antigen that self-assemble into nanoparticles did induce *anti*-ELP IgM and IgG, though no T cell responses were seen [35]. Therefore, antibody responses against pZ_R-ELP in OVA protein vesicles were also analyzed in this study. IgG1 antibody against pZ_R-ELP was detected after prime and boost immunization and IgG2a antibody response was detected after boost immunization (Fig. 6). Though pZ_R-ELP (33.8 μg) was given at a higher dose than OVA-Z_E (10 μg), both IgG1 and IgG2a antibody responses against OVA were significantly higher than against pZ_R-ELP. As OVA antigens were presented on the surface and pZ_R-ELP proteins were shielded by OVA-Z_E and embedded inside of the protein vesicles, OVA had higher chance to be processed and presented by APCs than pZ_R-ELP. Additionally, in a study by Cho et al., immune-tolerant ELPs were designed using atypical ELP sequences derived from homologous mouse and human elastin sequences [76]. As a result, ELPs themselves were not immunogenic in mice while ELP fused with OVA peptide enhanced antibody titers and cytotoxic T lymphocyte responses. If the immunogenicity of pZ_R-ELP needs to be diminished in future work, the natural sequence from mouse tropoelastin and human elastin can be employed to further reduce antibody responses against pZ_R-ELP. The fact that vesicle vaccine boost improved anti-OVA titers suggests that neutralization from the low titers of anti-pZ_R-ELP is not significant. Additionally, a recent report comparing antigen and scaffold antibody responses of *de novo* designed two-component protein cages found that anti-scaffold antibodies do not negatively correlate with anti-antigen responses for a panel of common viral antigens, except subdominant HIV-1 Env antigen [77].

3.5. OVA-specific T cell responses

Higher IgG2a antibody titers induced by the vesicle group suggested there was also a T cell response to OVA protein vesicles [78]. Mice were sacrificed 2 weeks after boost immunization and spleens were collected to analyze OVA-specific $CD3^+$ T cell responses. Isolated splenocytes were stimulated with OVA peptide cocktail and production of IFN-γ and

Experimental plan					
Date	Day 0	Day 14	Day 21	Day 33	Day 34
Procedure	Prime shot	Blood sample	Boost shot	Blood sample	Collect spleen

Fig. 4. Experimental plan of immunization and sample collection.

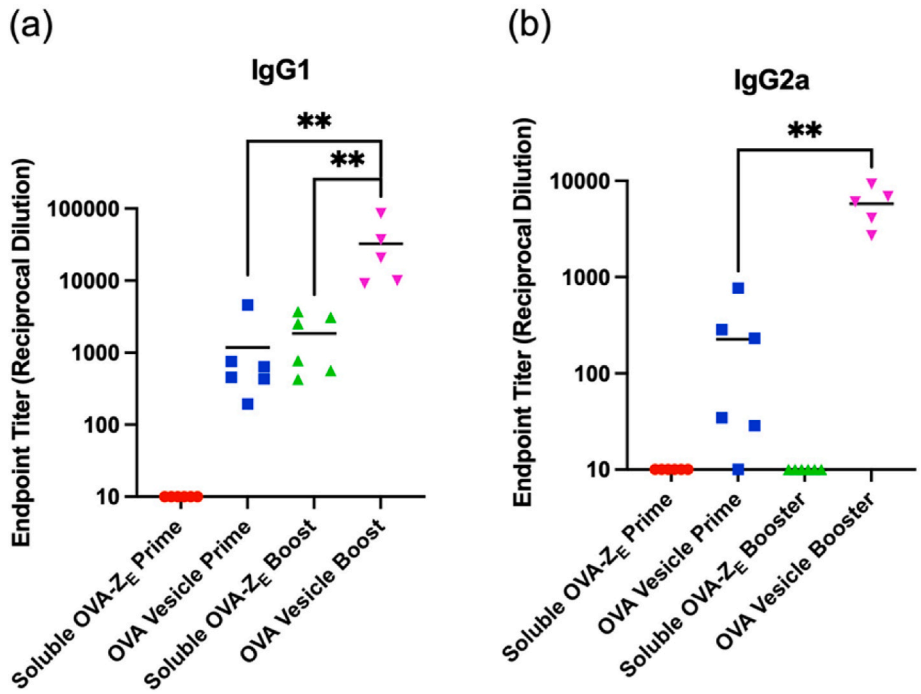

Fig. 5. ELISA endpoint titers of OVA specific IgG1 (a) and IgG2a (b) antibodies after prime and boost immunization. Each mouse was immunized with 10 μg OVA-Z_E in both soluble OVA-Z_E group and OVA protein vesicle group. Titer values too low for detection were arbitrarily set at 10. (**$p < 0.01$).

IL-4 cytokines by $CD4^+$ and $CD8^+$ splenocytes was measured (Fig. 7). The OVA protein vesicle group produced significantly higher amounts of IL-4 in $CD4^+$ T cells and both IFN-γ and IL-4 in $CD8^+$ T cells than the soluble OVA-Z_E group. The ELP-birch pollen antigen micelles also induced IL-4 production similar to alum adjuvanted antigen in lymph node T cells, though no other cytokine levels were increased [38]. In T cell subsets of splenocytes, Type 2 T helper (Th2) cell is associated with IL-4 production, and Th1 is associated with IFN-γ production [79]. Th2 cytokine IL-4 promotes B cells to produce IgG1 but inhibits IgG2a production, while Th1 cytokine IFN-γ enhances IgG2a production but inhibits IgG1. As shown in our data, significantly higher levels of IL-4 in $CD4^+$ cells corresponded with higher IgG1 antibody titer. Both humoral and cellular immune responses indicated that OVA protein vesicles induced Th2-biased responses. This is expected for OVA, which is an allergen not a pathogen and elicits a Th2 response when presented in its native conformation [80,81]. OVA conjugated onto the surface of micelles was reported to induce production of high IgG1 titer with relatively low IgG2a titer [82].

4. Conclusion

This work demonstrates the potential of protein vesicles as a subunit vaccine delivery platform. OVA protein vesicles were self-assembled from antigen fusion protein, OVA-Z_E, and thermoresponsive, photocrosslinkable protein, pZ_R-ELP. Protein vesicles showed the ability to display full-size antigens on the surface while maintaining the ability to self-assemble, which has not commonly been seen in other self-assembling systems. Immunization of mice proved that OVA protein vesicles induced OVA-specific humoral and cellular immune responses appropriate for conformational OVA allergen. Additionally, OVA vesicle stability outside the cold chain could be valuable for translation to all communities. Altogether, the protein vesicle is a promising vaccine platform given its ability to display antigen proteins, long-term stability, tunable size and multivalency, combined with its vaccination efficacy in mice. Previous work has demonstrated that protein vesicles can be made from globular proteins with a wide range of size and surface charge [56]. In future work, antigen proteins from pathogens will be incorporated into protein vesicles to examine the efficiency of protein vesicles to

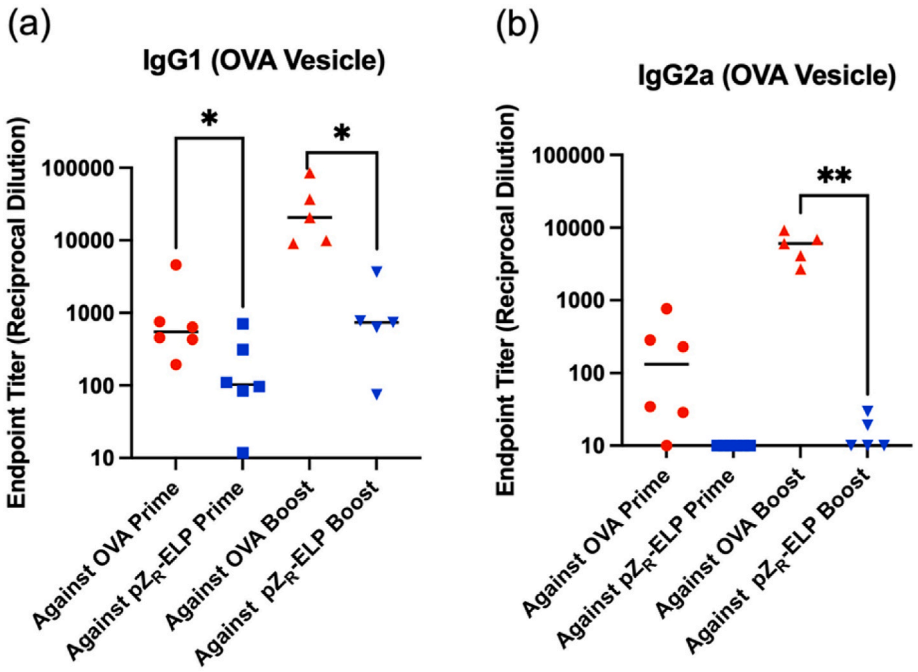

Fig. 6. Comparison of ELISA endpoint titers of IgG1 (a) and IgG2a (b) against OVA antigen and pZ_R-ELP antigen. Titer values too low for detection were arbitrarily set at 10. Data labeled "Against OVA" in red is replotted from Fig. 5 to compare with the titers against pZ_R-ELP. (**$p < 0.01$, *$p < 0.05$). (For interpretation of the references to colour in this figure legend, the reader is referred to the Web version of this article.)

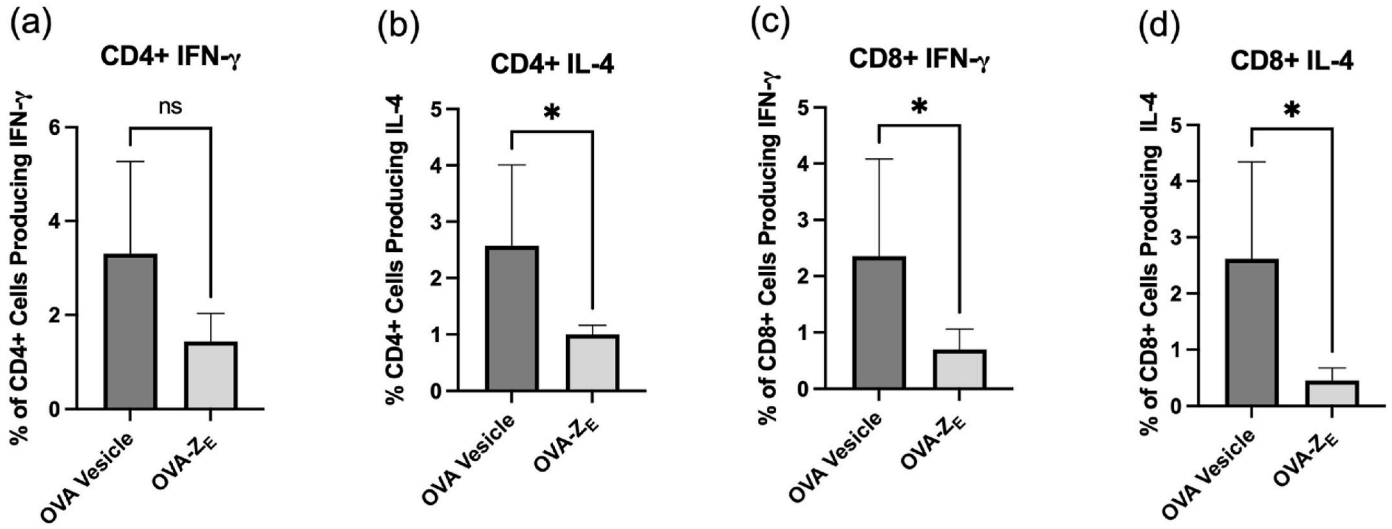

Fig. 7. Cytokine production in splenic T cells. Percent of $CD4^+$ cells secreting IFN-γ (a) and IL4 (b). Percent of $CD8^+$ cells secreting IFN-γ (c) and IL4 (d). (*$p < 0.05$).

protect again infectious diseases, including simultaneous presentation of multiple antigens. The ability to control antigen density could enable investigation of fundamental questions regarding the effect of multivalent antigen density and spacing on BCR binding and activation. Given the high positive charge in Z_R and hydrophobic lumen with cargo capacity [43], incorporation of nucleic acid or small molecule adjuvants may be possible to further enhance immunogenicity of antigens or bias the nature of the immune response. The modularity and simplicity of protein vesicles could enable a variety of vaccine applications.

The authors have no competing interests to declare.

CRediT authorship contribution statement

Yirui Li: Conceptualization, Formal analysis, Investigation, Methodology, Writing – original draft, Writing – review & editing. **Mariela R. Rodriguez-Otero:** Investigation, Writing – review & editing. **Julie A. Champion:** Conceptualization, Project administration, Resources, Supervision, Writing – review & editing.

Declaration of competing interest

The authors declare the following financial interests/personal relationships which may be considered as potential competing interests: Julie A. Champion and Mariela R. Rodriguez-Otero report financial support was provided by National Science Foundation.

Data availability

Data will be made available on request.

Acknowledgements

The authors acknowledge financial support from the National Science Foundation BMAT Award 2104734. M.R.R.-O. is supported by a National Science Foundation Graduate Research Fellowship under Grant No.DGE-2039655. This work was performed in part at the Georgia Tech Institute for Electronics and Nanotechnology, a member of the National Nanotechnology Coordinated Infrastructure, which is supported by the National Science Foundation (Grant No. ECCS-2025462). The authors gratefully acknowledge Prof. D.A. Tirrell and Prof. K. Zhang for Z_E and Z_R-ELP genes and AF-IQ *E. coli*. We acknowledge the contributions of named and unnamed people whose health, lives, livelihoods, legacy, and privacy were extorted, often without compensation, consent, or regard to their safety, in the name of biomedical research. These men, women, and children were stripped of their humanity, and often their identity. We knowingly use resources and knowledge with the gratitude and respect not given previously. We commit to educating ourselves and others on the history and ethical failures of biomedical research, expressing our gratitude, and encouraging others to do the same.

Appendix A. Supplementary data

Supplementary data to this article can be found online at https://doi.org/10.1016/j.biomaterials.2024.122666.

References

[1] B. Greenwood, The contribution of vaccination to global health: past, present and future, Philos. Trans. R. Soc. Lond. B Biol. Sci. 369 (1645) (2014) 20130433.
[2] S. Plotkin, History of vaccination, Proc. Natl. Acad. Sci. U. S. A. 111 (34) (2014) 12283–12287.
[3] P.D. Minor, Live attenuated vaccines: historical successes and current challenges, Virology 479–480 (2015) 379–392.
[4] R.J. Cox, K.A. Brokstad, P. Ogra, Influenza virus: immunity and vaccination strategies. Comparison of the immune response to inactivated and live, attenuated influenza vaccines, Scand. J. Immunol. 59 (1) (2004) 1–15.
[5] J.T. Schiller, D.R. Lowy, Raising expectations for subunit vaccine, J. Infect. Dis. 211 (9) (2015) 1373–1375.
[6] P.M. Moyle, I. Toth, Modern subunit vaccines: development, components, and research opportunities, ChemMedChem 8 (3) (2013) 360–376.
[7] Y. Perrie, et al., Vaccine adjuvant systems: enhancing the efficacy of sub-unit protein antigens, Int. J. Pharm. 364 (2) (2008) 272–280.
[8] M.L. De Temmerman, et al., Particulate vaccines: on the quest for optimal delivery and immune response, Drug Discov. Today 16 (13–14) (2011) 569–582.
[9] L. Zhao, et al., Nanoparticle vaccines, Vaccine 32 (3) (2014) 327–337.
[10] D.J. Irvine, et al., Synthetic nanoparticles for vaccines and immunotherapy, Chem. Rev. 115 (19) (2015) 11109–11146.
[11] A. Gregory, D. Williamson, R. Titball, Vaccine delivery using nanoparticles, Front. Cell. Infect. Microbiol. 3 (2013).
[12] A.K. Giddam, et al., Liposome-based delivery system for vaccine candidates: constructing an effective formulation, Nanomedicine (Lond) 7 (12) (2012) 1877–1893.
[13] R.J. Nevagi, M. Skwarczynski, I. Toth, Polymers for subunit vaccine delivery, Eur. Polym. J. 114 (2019) 397–410.
[14] A.N. Tsoras, J.A. Champion, Protein and peptide biomaterials for engineered subunit vaccines and immunotherapeutic applications, Annu. Rev. Chem. Biomol. Eng. 10 (1) (2019) 337–359.
[15] W. Jiang, et al., Biodegradable poly(lactic-co-glycolic acid) microparticles for injectable delivery of vaccine antigens, Adv. Drug Deliv. Rev. 57 (3) (2005) 391–410.
[16] S. Bobbala, S. Hook, Is there an optimal formulation and delivery strategy for subunit vaccines? Pharmaceut. Res. 33 (9) (2016) 2078–2097.
[17] M.B. Laurens, RTS,S/AS01 vaccine (Mosquirix™): an overview, Hum. Vaccines Immunother. 16 (3) (2020) 480–489.
[18] D.M. Harper, L.R. DeMars, HPV vaccines - a review of the first decade, Gynecol. Oncol. 146 (1) (2017) 196–204.
[19] M. Tarhini, et al., Protein-based nanoparticle preparation via nanoprecipitation method, Materials 11 (3) (2018).
[20] C. Weber, et al., Desolvation process and surface characterisation of protein nanoparticles, Int. J. Pharm. 194 (1) (2000) 91–102.
[21] J. López-Sagaseta, et al., Self-assembling protein nanoparticles in the design of vaccines, Comput. Struct. Biotechnol. J. 14 (2016) 58–68.
[22] C. Morris, et al., A modular vaccine platform combining self-assembled peptide cages and immunogenic peptides, Adv. Funct. Mater. 29 (8) (2019) 1807357.
[23] C.P. Karch, et al., The use of a P. falciparum specific coiled-coil domain to construct a self-assembling protein nanoparticle vaccine to prevent malaria, J. Nanobiotechnol. 15 (1) (2017) 62.
[24] C.P. Karch, et al., Design and characterization of a self-assembling protein nanoparticle displaying HIV-1 Env V1V2 loop in a native-like trimeric conformation as vaccine antigen, Nanomed. Nanotechnol. Biol. Med. 16 (2019) 206–216.
[25] C.P. Karch, et al., Vaccination with self-adjuvanted protein nanoparticles provides protection against lethal influenza challenge, Nanomed. Nanotechnol. Biol. Med. 13 (1) (2017) 241–251.
[26] C.P. Karch, et al., Vaccination with self-adjuvanted protein nanoparticles provides protection against lethal influenza challenge, Nanomedicine 13 (1) (2017) 241–251.
[27] M.W. Moore, F.R. Carbone, M.J. Bevan, Introduction of soluble protein into the class I pathway of antigen processing and presentation, Cell 54 (6) (1988) 777–785.
[28] B.A. Heesters, R.C. Myers, M.C. Carroll, Follicular dendritic cells: dynamic antigen libraries, Nat. Rev. Immunol. 14 (7) (2014) 495–504.
[29] J. Marcandalli, et al., Induction of potent neutralizing antibody responses by a designed protein nanoparticle vaccine for respiratory syncytial virus, Cell 176 (6) (2019) 1420–1431.e17.
[30] A.C. Walls, et al., Elicitation of potent neutralizing antibody responses by designed protein nanoparticle vaccines for SARS-CoV-2, Cell 183 (5) (2020) 1367–1382.e17.
[31] M.G. Joyce, et al., SARS-CoV-2 ferritin nanoparticle vaccines elicit broad SARS coronavirus immunogenicity, Cell Rep. 37 (12) (2021) 110143.
[32] D.W. Urry, Physical chemistry of biological free energy transduction as demonstrated by elastic protein-based polymers, J. Phys. Chem. B 101 (51) (1997) 11007–11028.
[33] D.W. Urry, et al., Temperature of polypeptide inverse temperature transition depends on mean residue hydrophobicity, J. Am. Chem. Soc. 113 (11) (1991) 4346–4348.
[34] D.W. Urry, et al., Hydrophobicity scale for proteins based on inverse temperature transitions, Biopolymers 32 (9) (1992) 1243–1250.
[35] C. García-Arévalo, et al., Immunomodulatory nanoparticles from elastin-like recombinamers: single-molecules for tuberculosis vaccine development, Mol. Pharm. 10 (2) (2013) 586–597.
[36] S. Cho, et al., Immune-tolerant elastin-like polypeptides (iTEPs) and their application as CTL vaccine carriers, J. Drug Target. 24 (4) (2016) 328–339.
[37] R.S. Ingrole, et al., Synthesis and Immunogenicity Assessment of Elastin-Like Polypeptide-M2e Construct as an Influenza Antigen, Nano LIFE 4 (2) (2014) 1450004.
[38] J. van Strien, et al., Bet V 1-displaying Elastin-like Polypeptide Nanoparticles Induce a Strong Humoral and Weak CD4+ T-Cell Response against Bet V 1 in a Murine Immunogenicity Model, 13, 2022 1006776.
[39] W.M. Park, J.A. Champion, Thermally triggered self-assembly of folded proteins into vesicles, J. Am. Chem. Soc. 136 (52) (2014) 17906–17909.
[40] D.R. Dautel, J.A. Champion, Protein vesicles self-assembled from functional globular proteins with different charge and size, Biomacromolecules 22 (1) (2020) 116–125 (2020).
[41] J.R. Moll, et al., Designed heterodimerizing leucine zippers with a ranger of pIs and stabilities up to 10(-15) M, Protein Sci. 10 (3) (2001) 649–655.
[42] J. Yeongseon, et al., Engineering globular protein vesicles through tunable self-assembly of recombinant fusion proteins, Small 13 (36) (2017) 1700399.
[43] Y. Li, J.A. Champion, Photocrosslinked, tunable protein vesicles for drug delivery applications, Adv. Healthcare Mater. 10 (15) (2021) 2001810.
[44] T.Z. Chang, et al., Effects of ovalbumin protein nanoparticle vaccine size and coating on dendritic cell processing, Biomater. Sci. 5 (2) (2017) 223–233.
[45] J.T. Wilson, et al., pH-responsive nanoparticle vaccines for dual-delivery of antigens and immunostimulatory oligonucleotides, ACS Nano 7 (5) (2013) 3912–3925.
[46] T.Z. Chang, et al., Host- and pathogen-derived adjuvant coatings on protein nanoparticle vaccines, Bioeng Transl Med 2 (1) (2017) 120–130.
[47] D. Datta, et al., A designed phenylalanyl-tRNA synthetase variant allows efficient in vivo incorporation of aryl ketone functionality into proteins, J. Am. Chem. Soc. 124 (20) (2002) 5652–5653.
[48] K. Kirshenbaum, I.S. Carrico, D.A. Tirrell, Biosynthesis of proteins incorporating a versatile set of phenylalanine analogues, Chembiochem 3 (2–3) (2002) 235–237.
[49] K. Zhang, M.R. Diehl, D.A. Tirrell, Artificial polypeptide scaffold for protein immobilization, J. Am. Chem. Soc. 127 (29) (2005) 10136–10137.
[50] P. Malyala, M. Singh, Endotoxin limits in formulations for preclinical research, J Pharm Sci 97 (6) (2008) 2041–2044.
[51] J.R. Crowther, The ELISA guidebook, Methods Mol. Biol. 149 (2000) 1–413. Iii-iv.
[52] J. Lobstein, et al., SHuffle, a novel Escherichia coli protein expression strain capable of correctly folding disulfide bonded proteins in its cytoplasm, Microb. Cell Factories 11 (1) (2012) 753.
[53] L. Deng, et al., Double-layered protein nanoparticles induce broad protection against divergent influenza A viruses, Nat. Commun. 9 (1) (2018) 359.
[54] R. Schwyzer, M. Caviezel, p-Azido-L-phenylalanine: a photo-affinity 'probe' related to tyrosine, Helv. Chim. Acta 54 (5) (1971) 1395–1400.
[55] Y. Cho, et al., Effects of hofmeister anions on the phase transition temperature of elastin-like polypeptides, J. Phys. Chem. B 112 (44) (2008) 13765–13771.
[56] D.R. Dautel, J.A. Champion, Protein vesicles self-assembled from functional globular proteins with different charge and size, Biomacromolecules 22 (1) (2021) 116–125.

[57] Y. Li, et al., Rational design of elastin-like polypeptide fusion proteins to tune self-assembly and properties of protein vesicles, J. Mater. Chem. B 11 (27) (2023) 6443–6452.
[58] Q. Lin, Q. Zhao, B. Lev, Cold chain transportation decision in the vaccine supply chain, Eur. J. Oper. Res. 283 (1) (2020) 182–195.
[59] B.F. Hibbs, et al., Safety of vaccines that have been kept outside of recommended temperatures: reports to the vaccine adverse event reporting system (VAERS), 2008-2012, Vaccine 36 (4) (2018) 553–558.
[60] K.D. Brune, M. Howarth, New routes and opportunities for modular construction of particulate vaccines: stick, click, and glue, Front. Immunol. 9 (2018).
[61] P.J.M. Brouwer, et al., Enhancing and shaping the immunogenicity of native-like HIV-1 envelope trimers with a two-component protein nanoparticle, Nat. Commun. 10 (1) (2019) 4272.
[62] R. Rahikainen, et al., Overcoming symmetry mismatch in vaccine nanoassembly through spontaneous amidation, Angew. Chem. Int. Ed. 60 (1) (2021) 321–330.
[63] T.K. Tan, et al., A COVID-19 vaccine candidate using SpyCatcher multimerization of the SARS-CoV-2 spike protein receptor-binding domain induces potent neutralising antibody responses, Nat. Commun. 12 (1) (2021) 542.
[64] W.-Y. Chan, et al., A novel, multiple-antigen pneumococcal vaccine protects against lethal Streptococcus pneumoniae challenge, Infect. Immun. 87 (3) (2019), 00846-18.
[65] F. Zhang, Y.-J. Lu, R. Malley, Multiple antigen-presenting system (MAPS) to induce comprehensive B- and T-cell immunity, Proc. Natl. Acad. Sci. USA 110 (33) (2013) 13564–13569.
[66] A. Impagliazzo, et al., A stable trimeric influenza hemagglutinin stem as a broadly protective immunogen, Science 349 (6254) (2015) 1301–1306.
[67] D.M. Eckert, V.N. Malashkevich, P.S. Kim, Crystal structure of GCN4-pIQI, a trimeric coiled coil with buried polar residues11Edited by P.E. Wright, J. Mol. Biol. 284 (4) (1998) 859–865.
[68] T. Storni, et al., Immunity in response to particulate antigen-delivery systems, Adv. Drug Deliv. Rev. 57 (3) (2005) 333–355.
[69] C. Théry, S. Amigorena, The cell biology of antigen presentation in dendritic cells, Curr. Opin. Immunol. 13 (1) (2001) 45–51.
[70] A. Gutjahr, et al., Biodegradable polymeric nanoparticles-based vaccine adjuvants for lymph nodes targeting, Vaccines 4 (4) (2016) 34.
[71] T. Uto, et al., Modulation of innate and adaptive immunity by biodegradable nanoparticles, Immunol. Lett. 125 (1) (2009) 46–52.
[72] D.J. Irvine, B.J. Read, Shaping humoral immunity to vaccines through antigen-displaying nanoparticles, Curr. Opin. Immunol. 65 (2020) 1–6.
[73] D.W. Urry, et al., Biocompatibility of the bioelastic materials, poly(GVGVP) and its γ-irradiation cross-linked matrix: summary of generic biological test results, J. Bioact. Compat Polym. 6 (3) (1991) 263–282.
[74] C.A. Gilroy, K.M. Luginbuhl, A. Chilkoti, Controlled release of biologics for the treatment of type 2 diabetes, J. Contr. Release : official journal of the Controlled Release Society 240 (2016) 151–164.
[75] F.S. Nouri, et al., Reducing the visibility of the vector/DNA nanocomplexes to the immune system by elastin-like peptides, Pharmaceut. Res. 32 (9) (2015) 3018–3028.
[76] S. Cho, et al., Immune-tolerant elastin-like polypeptides (iTEPs) and their application as CTL vaccine carriers, J. Drug Target. 24 (4) (2016) 328–339.
[77] J.C. Kraft, et al., Antigen- and scaffold-specific antibody responses to protein nanoparticle immunogens, Cell Rep Med 3 (10) (2022) 100780.
[78] P.K. Mongini, K.E. Stein, W.E. Paul, T cell regulation of IgG subclass antibody production in response to T-independent antigens, J. Exp. Med. 153 (1) (1981) 1–12.
[79] I. Raphael, et al., T cell subsets and their signature cytokines in autoimmune and inflammatory diseases, Cytokine 74 (1) (2015) 5–17.
[80] J.M. Spergel, et al., Epicutaneous sensitization with protein antigen induces localized allergic dermatitis and hyperresponsiveness to methacholine after single exposure to aerosolized antigen in mice, J. Clin. Invest. 101 (8) (1998) 1614–1622.
[81] P. Avci, et al., Animal models of skin disease for drug discovery, Expet Opin. Drug Discov. 8 (3) (2013) 331–355.
[82] N. Yanase, et al., OVA-bound nanoparticles induce OVA-specific IgG1, IgG2a, and IgG2b responses with low IgE synthesis, Vaccine 32 (45) (2014) 5918–5924.